Interactive Boundary Layer [IBL]
or
Inviscid-Viscous Interactions [IVI or VII]

P.-Y. Lagrée
CNRS & UPMC Univ Paris 06, UMR 7190,
Institut Jean Le Rond ∂'Alembert, Boîte 162, F-75005 Paris, France
pierre-yves.lagree@upmc.fr ; www.lmm.jussieu.fr/∼lagree

October 29, 2015

Abstract

We present here the Interacting Boundary Layer Theory. This is a way to solve an approximation of the Navier Stokes equations using the Ideal Fluid Boundary / Layer decomposition. But, instead of solving first the ideal Fluid and second the Boundary Layer, both are solved together. This "strong coupling" allows to compute separated flows which was impossible with the classical way. We present some numerical experiments.

1 Introduction

We are now familiar with the concept of Ideal Fluid/ Boundary Layer decomposition. We have understood, that putting first $1/Re = 0$ in Navier Stokes gives the Euler description. In this non viscous description, the flow slips at the wall. This gives an outer velocity at the wall, parallel to the wall. This singular behavior is removed by the introduction of a thin layer of relative thickness $1/\sqrt{Re}$. The velocity at the upper bound at infinity is by matching the ideal fluid velocity at the wall. In this boundary layer, viscous effects act in order to decrease this velocity to full fit the no slip condition.

From a practical aeronautical point of view, the ideal fluid description gives the lift of the wing, the viscous layer gives the drag (we are aware of the induced drag on finite span wings which is a ideal fluid effect).

But, everything is not so simple, there are problems when computing the boundary layer: we remain again the boundary layer separation problem. But there are other paradoxes: we introduce an other important problem which is the "upstream influence problem". We will show that to solve those two problems, the good strategy is a strategy of "strong interaction" between the boundary layer and the ideal fluid. So it was called "Interacting Boundary Layer" or "Viscous Inviscid Interaction" (or Inviscid Viscous Interaction). Some practical examples from literature and for various flows régimes are presented.

2 Problems associated with the Boundary Layer

2.1 Separation

We already had a glimpse on the problem of separation of boundary layer. We saw that for a given external flow, one can not compute the boundary layer if the skin friction vanishes. This is called Goldstein singularity, close to the point of separation:

$$u = u_s(y) + \frac{\partial u_s}{\partial y} A(x) \quad v = -\frac{\partial A}{\partial x} u_s \quad A(x) = a\sqrt{x_s - x}.$$

So, for a given external decreasing velocity, there is a possibility of separation with a singularity. The computation can not pass the separation. Most of classical text book of fluid mechanics do the same and end their course on boundary layers by this dead end, for example one can read in Kundu [9]: "the boundary layer equations are valid only far downstream as the point of separation. Beyond it the boundary layer becomes so thick that the basic underlying assumptions become invalid. Moreover, the parabolic character of the boundary layer equations requires that a numerical integration is possible only in the direction of advection (along which information are propagated), which is *upstream* within the reversed flow region. A forward (downstream) integration of the boundary layer equations therefore breaks down after the separation point. Last, we can no longer apply potential theory to find the pressure distribution in the separation region, as the effective boundary of the irrotational flow is no longer the solid surface but some unknown shape encompassing part of the body plus the separation region."

Is it a dead end? No!

2.2 Inverse Boundary Layer

This paragraph must be reversed! In fact computing the reverse flow within a boundary layer is possible with the Prandtl equations. The good idea is: impose the displacement thickness and solve for pressure gradient. This was the idea of Catherall and Mangler [3] in 66, and they were the first to succeeded to pass the point of flow separation while solving the steady boundary-layer equations with a prescribed displacement thickness (a kind of parabolic shape).

Does it surprise us? We have already solved the Falkner Skan equations: we obtained flow separation for some values of β. To obtain it, we had to impose the thickness $\int_0^\infty (1-f')d\eta$, and we found the value of β associated. Hence, a simple way to feel that the boundary layer must be solved in inverse way is really the Falkner Skan case. It is representative by many aspects of the boundary layer behavior: for a given external velocity one has a given β and one computes the corresponding profile. But, we see on figure 1 that if the external velocity is with a β to small, there is no solution. Only for an *ad hoc* external velocity we have solution(s).

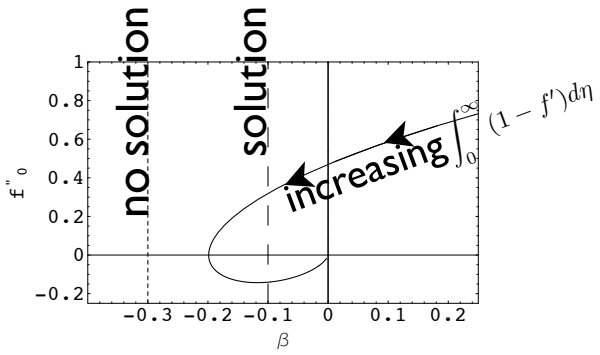

Figure 1: Not any external velocity is compatible with the boundary layer, for example in the Falkner Skan case, too small β (less than -0.199) are not relevant (small dashing). A larger value of the outer velocity gradient (large dashing) gives solutions.

See on figure 2 an example of inverse boundary layer computation using the Keller Box method, the displacement δ_1 is given, the velocity is deduced.

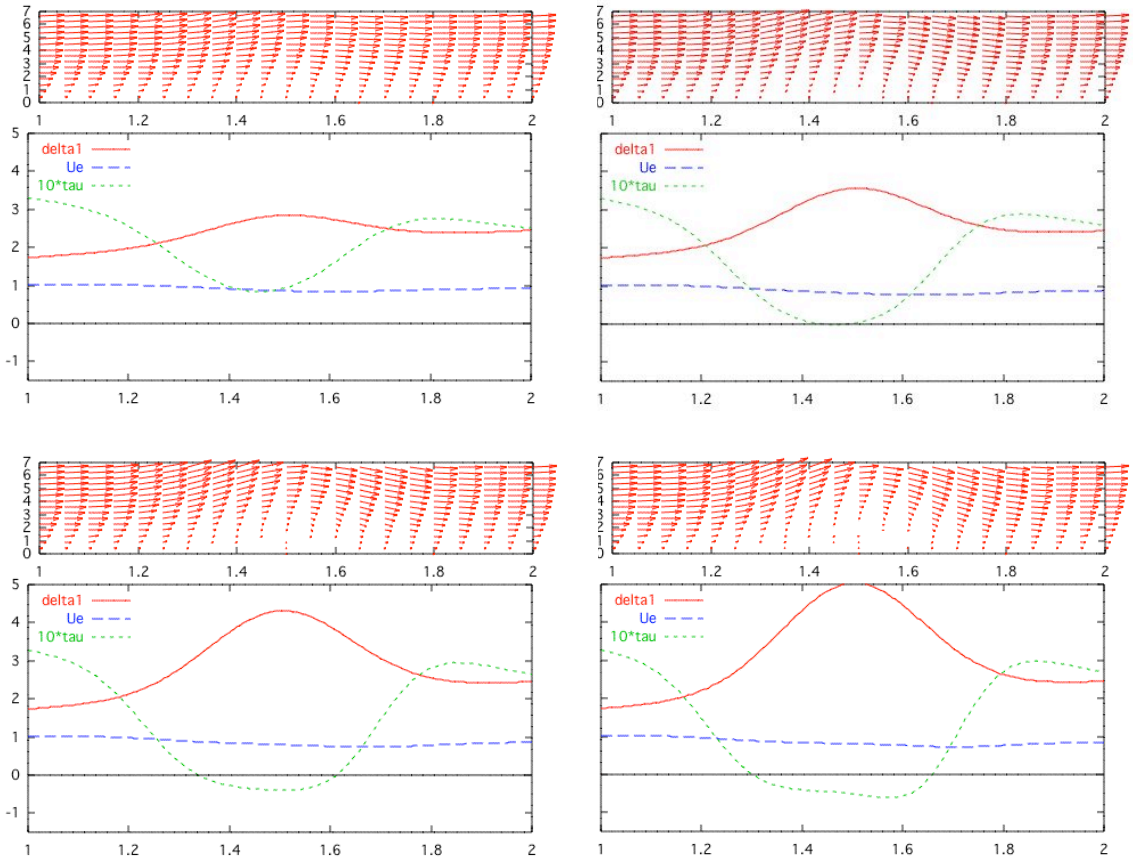

Figure 2: Examples of inverse boundary layer computation. Separation is not an issue when displacement is prescribed. Here given $\tilde{\delta}_1 = 1.73\bar{x}^{1/2} + \alpha e^{-25(\bar{x}-1.5)^2}$, we compute the associated external velocity, and the skin friction. For $\alpha = 1.43$ (top right) is the incipient separation, for smaller increase of $\tilde{\delta}_1$, there is no separation just a decrease of velocity (top left). Bottom: for larger values we have separation with reverse flow. The outer velocity decreases and reincreases.

2.3 The problem of the influence of downstream on upstream

2.3.1 Observations, the paradox

One other strange problem appeared in the 50' at the time of the supersonic-conquest: the problem of "Upstream Influence". A model configuration for supersonic wing was the aligned flat plate in a compressible supersonic flow. In various experiments in supersonic flows (Ackeret Chapman and others), it was observed that an impinging shock wave on a boundary layer produces perturbations far upstream. The boundary layer deviates from its basic state upstream of the impinging shock, see on figure 3 from Stewartson 64 book [18]. On this figure we even see that three different accidents (an impinging shock, a forward facing step and a wedge) produce the same upstream flow. The deviation occurs far away (in boundary layer thickness units) from the accident.

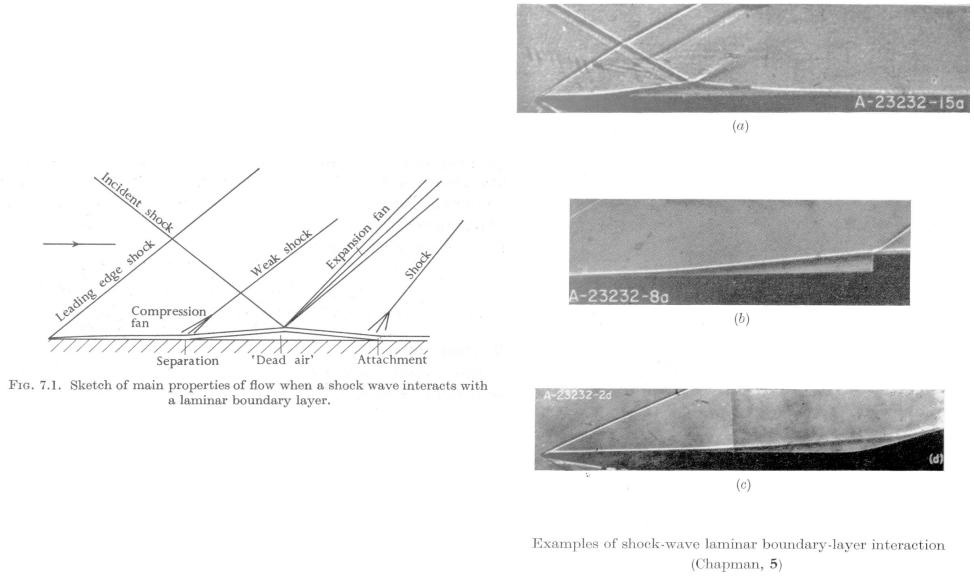

FIG. 7.1. Sketch of main properties of flow when a shock wave interacts with a laminar boundary layer.

Examples of shock-wave laminar boundary-layer interaction (Chapman, 5)

Figure 3: The "upstream influence" in supersonic flows. Left, a sketch of the shock wave boundary layer interaction. Right, the three different accidents (an impinging shock, a forward facing step and a wedge) produce the same upstream flow. Figures from Stewartson book [18].

In the classical supersonic framework this is impossible (figure 4). First the ideal fluid is supersonic (hyperbolic) so perturbations move downstream in the Mach cone. Second, the boundary layer is parabolic, so perturbations move downstream and across the boundary layer. No disturbance can theoretically move upstream against the flow. This is the upstream influence paradox.

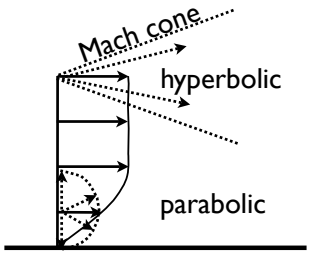

Figure 4: Upstream influence paradox: the ideal fluid is supersonic (hyperbolic, perturbations move downstream in the Mach cone), the boundary layer is parabolic (perturbations move downstream and across the boundary layer).

2.3.2 Some explanations

This puzzled people.

• Some people think that there is always a subsonic part in the boundary layer, so that the retroaction can travel back in this subsonic layer. In fact it is not the good mechanism as the the upstream influence would be of same length than this subsonic layer is thick. But on the experiments, the longitudinal scale is far larger than the boundary layer thickness.

• Garvine [8] proposed a simplified boundary layer model linearising around $u = 1$ the supersonic boundary layer (neglecting thermal effects):

$$\partial_{\bar{x}}\tilde{u} = -\partial_{\bar{x}}\bar{p} + \partial^2_{\tilde{y}}\tilde{u}, \quad \tilde{v} = -\int_0^{\tilde{y}} \partial_{\bar{x}}\tilde{u} d\tilde{y}$$

and writing the Ackeret formula as:

$$\bar{p} = \frac{M^2}{\sqrt{Re}\sqrt{M^2-1}}\tilde{v}(\tilde{\delta})$$

he obtains after claiming $\tilde{\delta} = cst$ (yes he did!) that the pressure gradient is $-\frac{M^2}{\sqrt{Re}\sqrt{M^2-1}}\int_0^{\tilde{\delta}} \tilde{u}_{\bar{x}\bar{x}} d\tilde{y}$ so that a model equation of the interaction is:

$$\partial_{\bar{x}}\tilde{u} = \frac{M^2}{\sqrt{Re}\sqrt{M^2-1}}\int_0^{\delta} u_{\bar{x}\bar{x}} d\tilde{y} + \partial^2_{\tilde{y}}\tilde{u}.$$

It pointed out the come back of ellipticity due to this $u_{\bar{x}\bar{x}}$ term. He then obtained a set of eigen solutions with Laplace transform, in fact the exponentially growing one of those solutions can be obtained in looking to $e^{K\bar{x}}$ solutions, so that solution behaves as:

$$e^{\frac{\sqrt{Re}\sqrt{M^2-1}}{M^2\tilde{\delta}}\bar{x}}.$$

So the coupling of the two equations produces explosive solutions.

• Numerically those explosive solutions were obtained by Werle Dwoyer, and Hankey [19] (among others). On figure 5 we have a clear example of what happens when solving in a marching way the coupled system. Starting from a given initial location they solved the coupled boundary layer system with the so called tangent wedge law (valid for stronger shocks than the linearised Ackeret formula). They showed that changing a bit one parameter may cause different solutions. Those are called "branching solutions".

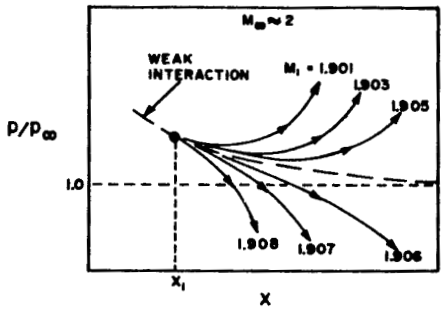

Figure 5: Branching solutions [19]: changing a bit one parameter may cause different solutions while solving the equations with a marching scheme.

• In fact, one may consider the most simple argument, see Le Balleur [12]. He considers the strong coupling of the boundary layer in Von Kármán form (neglecting again thermal effects) with the Ackeret formula

(linking the perturbation of pressure at $M > 1$ due to the variations of the effective wall (represented by δ_1) as:

$$\frac{d}{d\bar{x}}(\frac{\tilde{\delta}_1}{H}) + \frac{\tilde{\delta}_1}{\bar{u}_e}(1+\frac{2}{H})\frac{d\bar{u}_e}{d\bar{x}} = \frac{f_2 H}{\tilde{\delta}_1 \bar{u}_e}, \;\; \bar{p} = \frac{M^2}{\sqrt{Re}\sqrt{M^2-1}}\frac{d\tilde{\delta}_1}{d\bar{x}}, \tag{1}$$

so that, supposing that $\bar{u}_e$ is nearly one and $\partial_{\bar{x}}\bar{u}_e = -\partial_{\bar{x}}\bar{p}$

$$\frac{d}{d\bar{x}}(\frac{\tilde{\delta}_1}{H}) = \frac{\tilde{\delta}_1}{\bar{u}_e}(1+\frac{2}{H})\frac{M^2}{\sqrt{Re}\sqrt{M^2-1}}\frac{d^2\tilde{\delta}_1}{d\bar{x}^2} + \frac{f_2 H}{\tilde{\delta}_1 \bar{u}_e},$$

this equation is "not so far" from from the basic flow with subscript 0 and $\bar{u}_e \sim 1$, so after linearisation.

$$\frac{d}{d\bar{x}}\tilde{\delta}_1 = \frac{\tilde{\delta}_{10}}{\bar{u}_e}(H_0+2)\frac{M^2}{\sqrt{Re}\sqrt{M^2-1}}\frac{d^2\tilde{\delta}_1}{d\bar{x}^2} + ...$$

where we forget the contribution of the skin friction. So again, we obtain exponential solutions (called supercritical by Crocco and Lees in 52) for the disturbance of the displacement thickness δ_1:

$$e^{\frac{\sqrt{Re}\sqrt{M^2-1}}{\tilde{\delta}_{10}M^2(H_0+2)}\bar{x}}.$$

It is nearly the same result than Garvine.

• In fact, Lighthill in 53 proposed a pre-theory of triple deck explaining most of the mechanism (see in Stewartson 64 book as well). We will see it in the chapter on Triple Deck.

• This kind of solution will be called "self induced solution" in the Triple Deck framework. This upstream influence will be understood as a not well posed problem. In fact, even if each part of the flow seems hyperbolic/ parabolic, due to the interaction one recovers the output influence.

This is the case in the supersonic flows, in shallow water flows at small Froude number, in mixed convection. But there exist flows with no upstream influence: for example in the symmetrical pipe flows.

As a conclusion of this section, we see that the new ingredient is that the boundary layer is no more driven by the ideal fluid but can retroact. The retroaction explains the observed self induced interaction.

3 Interactive Boundary Layer

3.1 Examples of users

So it became clear that the interaction with the ideal fluid is not weak but strong. In the early 60 Gad and Curle employed Von Kármán -Pohlhausen method to try to solve the shock waves-boundary layer interaction, "without much success" (as quoted by Lees and Reeves [11]. Lees and Reeves in 64 [11] did computations with integral methods, with more success, but the details are not so clear. Reyhner Flügge Lotz 68 [17] did finite differences on the Boundary layer and succeed by iteration to compute the supersonic wedge interaction.

Among people working for applications in the aerospace area, some names are to be associated to IBL/ IVI. Among them:

• Le Balleur, from 1977 understood the interaction and using Von Kármán profiles did a lot of practical computations at ONERA, in supersonic and transsonic régimes.
• Veldman as well has is own codes at the National Aerospace Laboratory NLR in Amsterdam,
• Carter, Jameson at Stanford.
• Cebeci did a huge work (several books on the interactive boundary layer for example [4] [2]) and applied IVI at Boeing.
• Lock & Williams in a review [15], present the english RAE point of view.
• And last but not least Neiland and Sychev at the TsAGI in USSR.
Of course, this is a very very partial list.

3.2 Interactive Boundary Layer

One other way to bypass Goldstein singularity is to adopt the Interactive Boundary Layer point of view. It means that we use the classical Prantdl boundary layer equations :

$$\frac{\partial \tilde{u}}{\partial \bar{x}} + \frac{\partial \tilde{v}}{\partial \tilde{y}} = 0, \quad \tilde{u}\frac{\partial \tilde{u}}{\partial \bar{x}} + \tilde{v}\frac{\partial \tilde{u}}{\partial \tilde{y}} = \bar{u}_e \frac{d\bar{u}_e}{d\bar{x}} + \frac{\partial^2 \tilde{u}}{\partial \tilde{y}^2},$$

with no slip boundary conditions ($\tilde{u} = \tilde{v} = 0$ on the body $\bar{f}(\bar{x})$), a first given velocity profile: Blasius. The matching $\tilde{u}(\bar{x}, \tilde{y} \to \infty) \to \bar{u}_e(\bar{x})$.

A result of this computation is the transverse velocity at infinity, remember that for large $\tilde{y}$ the transverse velocity behaves as:

$$\tilde{v} \simeq \frac{d(\tilde{\delta}_1 \bar{u}_e)}{d\bar{x}} - \tilde{y}\frac{\partial \tilde{u}}{\partial \bar{x}}$$

which gives the "blowing velocity".

$$\bar{v}_e = Re^{-1/2}\frac{d(\tilde{\delta}_1 \bar{u}_e)}{d\bar{x}}$$

Hence, the outer flow is no more only given by the wall $\bar{f}(\bar{x})$ (so that the blowing velocity is $\bar{f}'\bar{u}_e$) but, the wall is "thickened" by the boundary layer thickness (or "blowing velocity", or "transpiration boundary condition"), so that for a subsonic flow:

$$\bar{u}_e = 1 + \frac{1}{\pi}\int \frac{\bar{f}'(\bar{x})\bar{u}_e + Re^{-1/2}\frac{d(\tilde{\delta}_1 \bar{u}_e)}{d\bar{x}}}{x - \xi} d\xi$$

or in a supersonic flow

$$\bar{u}_e = 1 - \frac{M^2}{\sqrt{M^2 - 1}}[\frac{d}{d\bar{x}}\bar{f}(\bar{x})\bar{u}_e + Re^{-1/2}\frac{d(\tilde{\delta}_1 \bar{u}_e)}{d\bar{x}}]$$

Instead of the usual weak coupling with the hierarchy (figure 6 left), the boundary layer retroacts on the ideal fluid (figure 6 right). The boundary layer thickness δ_1 acts as a fictive wall (cf figure 21 of chapter

second order), it disturbs the ideal fluid, the pressure (pressure and velocity $\bar{u}_e(\bar{x})$ are linked) develops the boundary layer itself. It is a strong interaction. The two layers are coupled. It explains the term "Interactive Boundary Layer", or "Viscous Inviscid Interaction".

Most of the separation problems are then solved...

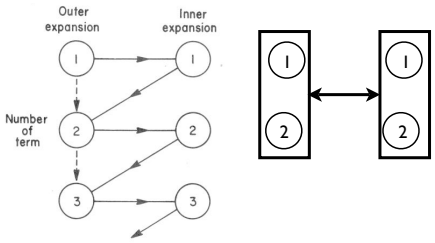

Figure 6: Interactive Boundary Layer, left the usual point of view of the "regular development ". Right, we mix the terms, as there is a singular behavior : $Re^{-1/2}\frac{d(\tilde{\delta}_1\bar{u}_e)}{d\bar{x}}$ is not so small...

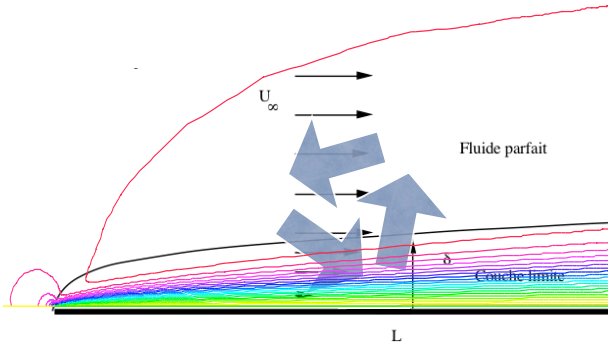

Figure 7: Interactive Boundary Layer

3.3 Justification of the Interactive Boundary Layer

At separation, the displacement boundary layer thickness becomes very thick. It is then not counterintuitive to think that the ideal fluid will be drastically changed by the the viscous layer. That is the picture for "Triple Deck", but the scales are changed.

In fact one may say that the problem consists to solve ideal fluid up to $1/Re$:

$$\bar{u}_e = 1 + \frac{1}{\pi}\int \frac{\bar{f}'(\bar{x})\bar{u}_e + Re^{-1/2}\frac{d(\tilde{\delta}_1\bar{u}_e)}{d\bar{x}}}{x-\xi}d\xi + O(1/Re)$$

plus the Boundary Layer problems at order 0 and at order $1/\sqrt{Re}$ (to be consistent with the $O(1/Re)$.

The usual approximation supposes that the term $Re^{-1/2}\frac{d(\tilde{\delta}_1\bar{u}_e)}{d\bar{x}}$ is negligeable as $Re^{-1/2}\to 0$. This is the regular development point of view. But at separation, $\frac{d(\tilde{\delta}_1\bar{u}_e)}{d\bar{x}}$ is no more small, it is large. Hence one can not neglect $Re^{-1/2}\frac{d(\tilde{\delta}_1\bar{u}_e)}{d\bar{x}}$. This is again a singular perturbation.

In fact it is easy to show the that the IBL equations (*Interactive Boundary Layer Equations*) give at large Reynolds number the Triple Deck structure. The $-A$ is the disturbance of the displacement thickness.

The IBL equations seem to be ill posed as they mix different order of magnitude.

Starting from NS equations, Dechaume Mauss and Cousteix [6] and Cousteix & Mauss [5] showed that we may obtain the IBL system using an other technique than "Matched Asymptotic Expansion". They rather used the so called "Successive Complementary Expansions Method" (MASC in french).

3.4 Coupling the solvers

3.4.1 Boxes

As there are two problems, it is natural to define kind of "boxes". A first "box" is the Euler Solver. Given a wall, it computes the pressure and the slip velocity. This box may be a subsonic, supersonic... a linear or not solver. It does not matter, the input is the wall geometry, the output is the slip velocity.

The second "box" is of course the boundary layer box, given an outer velocity, it computes the displacement thickness. The equations may be laminar or turbulent with any turbulent model. It may be full finite differences resolution or Von Kármán integral method. This box may be used in reverse, given a displacement thickness it computes what outer velocity produces it.

3.4.2 Coupling

Now, we couple the boxes and present the various possibilities. In fact we will use δ_1 and u in the following figures. We may use $\frac{d\delta_1}{dx}$ instead of δ_1, and instead of u we may use $-p$ (by Bernoulli linearised) or we may use $\frac{dp}{dx}$. There is no real influence of the choice of δ_1 instead of his slope, nor in u, p or his gradient.

• Now, having those boxes, we have to branch them. First, the classical boundary layer theory may be represented as a ideal fluid box followed by a boundary layer box, figure 8.

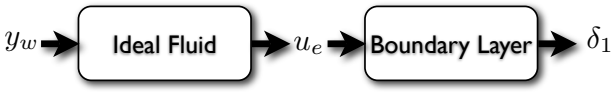

Figure 8: Classical Boundary layer, the geometry gives the velocity which gives the boundary layer.

• But as mentioned previously, branching the output of the boundary layer to the input of the ideal fluid will give the second order effects but will not allow the separation, figure 9.

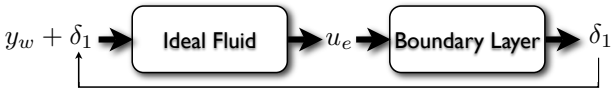

Figure 9: "Direct method": the geometry gives the velocity which gives the boundary layer, the rebranching will give the second order effects.

• The good way to solve the boundary layer, is to solve it in inverse, we can imagine that we solve the ideal fluid in inverse as well. This is the "inverse method" figure 10. in fact it is not a good idea as it is difficult to rewrite the Euler codes.

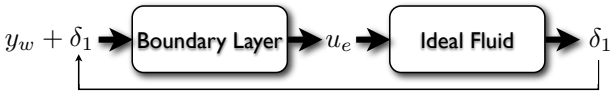

Figure 10: "Inverse method", the total geometry (boundary layer thickness and effective geometry) give the velocity which gives a total geometry, and so on.

• The good way to solve the boundary layer, is to solve it in inverse, the good way to solve the ideal fluid is in the direct way. So we have to relax the input depending on the difference of the outputs. This is the semi-inverse coupling by Le Balleur (figure 11).
• There are other possibilities, one is the "quasisimultaneous method". It means that during the coupling values computed downstream are reinjected, which is more useful in the subsonic case.

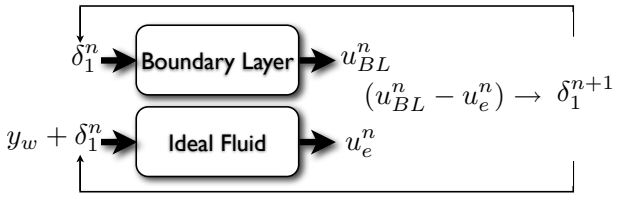

Figure 11: "Semi Inverse method", inverse boundary layer, direct ideal fluid. The difference of the two output velocities is used to update the displacement thickness, and so on.

3.4.3 Semi inverse coupling

The point to be clarified is how to update the new δ_1^{n+1} from δ_1^n and the difference $(u_{BL}^n - u_e^n)$, the simplest way is to write:

$$\delta^{n+1} = \delta^n + \lambda(u_{BL}^n - u_e^n)$$

One has to notice that by the Bernoulli relation variation of velocity are opposite of variation of pressure so that we can write as well:

$$\delta^{n+1} = \delta^n - \lambda(p_{BL}^n - p_e^n).$$

The choice of λ is such as we obtain stability for the iterative method.

Le Balleur (see [13] and Wigton and Holt [20]) analysis consist to linearize the equation. He defines two operators, one for each box, first B^* defined as $\delta^n = B^* p_{BL}^n$ and for the ideal fluid, he defines in the same vein a linear response $\delta^n = B p_e^n$. Then the update is as:

$$\delta^{n+1} = \delta^n - \lambda(1/B^* - 1/B)\delta^n$$

To make it clear, we use Fourier analysis for all the frequencies between π/L and $\pi/\Delta x$ (the smallest linked to the domain size, and the highest linked to the discretisation step). Furthermore, the B operator may be obtained in subsonic flow we have $B = -1/k$. The analysis is then very simple, defining a "gain" $G = \delta^{n+1}/\delta^n$:

$$G = 1 - \lambda(\frac{1}{B^*} + k),$$

we want $|G| < 1$ for $\pi/L < k < \pi/\Delta x$. Often ([13], [20]), it was considered that B^* was real, so we can find an optimal λ.

For a supersonic flow we have $B = (ik\sqrt{M^2}/(M^2-1))^{-1}$. It is easy to show that in this case it is impossible to find an optimal λ. The coupling is always unstable. The good coupling is now with the derivative of the pressure:

$$\delta^{n+1} = \delta^n - \mu(\frac{d}{dx}p_{BL}^n - \frac{d}{dx}p_e^n)$$

then again we have:

$$\delta^{n+1} = \delta^n - \mu ik(1/B^* - 1/B)\delta^n$$

which allows to define a "gain" $G = \delta^{n+1}/\delta^n$. We want $|G| < 1$ for all the space frequencies $\pi/L < k < \pi/\Delta x$. We can find an optimal μ.

In the following examples, we use this semi-inverse coupling.

4 Examples

4.1 Some numerical examples

We just reproduce here some examples from literature using this IBL theory. On the curves, the experimental and the computation are displayed showing a very good concordance. We selected among others comparisons of experiments, IBL and Ideal Fluid over an airfoil. We selected Drela & Giles [7] on figure 12, comparisons from Le Balleur computations 13, and comparisons from Lock & Williams [15] on figure 14. On figure 15, Aftosmis et al. [1] successfully compare IBL strategy with a Navier Stokes solver.

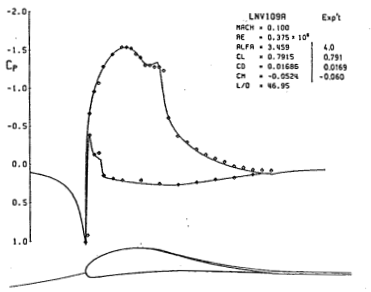

Fig. 9 LNV109A calculated and experimental pressure distributions.

Figure 12: Example of comparison of IBL computation, Drela & Giles [7]

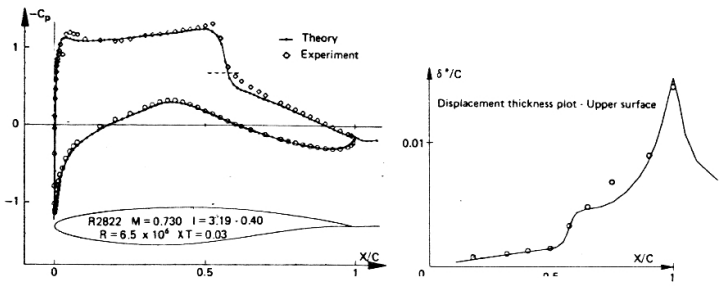

Figure 6. Transonic viscous solver at supercritical conditions (RAE 2822, $M = 0.730$, $\alpha = 2.79°$, $R = 6.5 \times 10^6$, $x_t = 0.03$).

Figure 13: Example of comparison of IBL computation, Le Balleur.

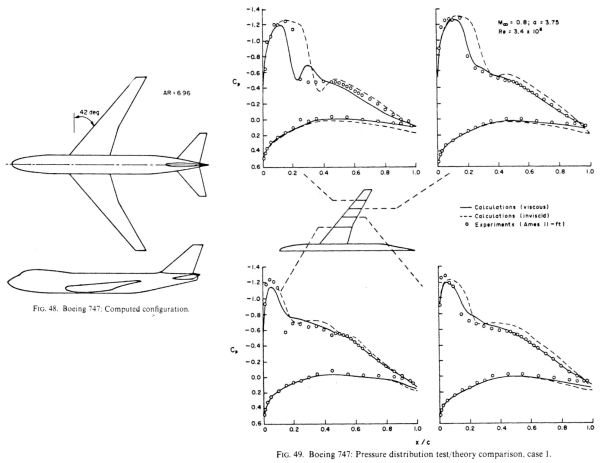

FIG. 48. Boeing 747: Computed configuration.

FIG. 49. Boeing 747: Pressure distribution test/theory comparison. case 1.

Figure 14: Example of comparison of IBL computation, Lock & Williams [15]

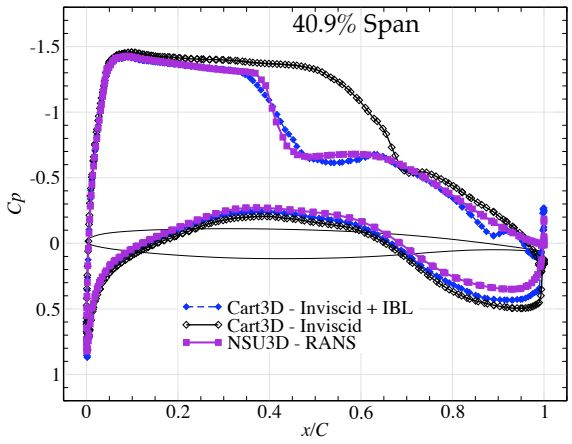

Figure 15: Example of comparison of IBL computation, pressures from [1] (coupled-IBL approach) compared with results from the pure inviscid solver and published data using the NSU3D RANS solver (see [1] for details).

4.2 Some numerical examples

4.2.1 Bump on a flat plate in a incompressible (subsonic) flow.

As a first example (fig 16), we present the results for the IBL on a flat plate with a bump defined by $\bar{y}_w = \alpha e^{-25(\bar{x}-2)^2}$; with α increasing by steps of 0.01 and $Re = 10000$. The velocity is:

$$\bar{u}_e = 1 + \frac{1}{\pi} \int \frac{\bar{f}'(\bar{x}) + Re^{-1/2} \frac{d(\tilde{\delta}_1 \bar{u}_e)}{d\bar{x}}}{x - \xi} d\xi$$

Before the bump there is a small decrease of the $\bar{u}_e$ velocity. In a pure Hilbert case, the response in $\bar{u}_e$ is perfectly symmetrical, but here, due to the boundary layer, the velocity is no more symmetrical. Due to the acceleration on the bump, the displacement thickness first decreases and increases again after the bump. It increases more. So, there is a small overshoot of the thickness associated with the boundary layer separation. This makes the outer velocity non symmetrical. The skin friction increases before the crest, and decreases after. This is consistent with the fact that, for instance, before the crest, the velocity increases, and the boundary layer thickness decreases, so the slope of the velocity in the boundary layer increases (it is more or less the ratio of $\bar{u}_e$ and $\tilde{\delta}_1$), the reverse happens after. We notice that the maximum of the skin friction is before the crest, after the inflexion point of the bump, the velocity increases less, but the boundary layer continues to decrease because of the inertia of the fluid, so the maximum of skin friction is between the inflexion point of the bump and the crest. There is eventually a separated bulb with negative skin friction.

4.2.2 Bump on a flat plate in a Supersonic flow.

As a second example (fig 17), we present the results for the IBL on a flat plate with a bump defined by $\bar{y}_w = \alpha e^{-25(\bar{x}-3.5)^2}$; but in the compressible supersonic case, so that the edge velocity is:

$$\bar{u}_e = 1 - \frac{M^2}{\sqrt{M^2 - 1}} [\frac{d}{d\bar{x}} \bar{f}(\bar{x}) + Re^{-1/2} \frac{d(\tilde{\delta}_1 \bar{u}_e)}{d\bar{x}}].$$

The bump creates upstream influence and a separated bulb far upstream. The skin friction reincreases and then redecreases to create a second separated bulb.

4.2.3 Bump on a flat plate in subcritical flow.

Nearly the same occurs in the case of the subcritical flow ($F < 1$) or in the case of symmetrical pipe flows. The edge velocity is:

$$\bar{u}_e = 1 + \frac{1}{1 - F} [\bar{f}(\bar{x}) + \tilde{\delta}_1 Re^{-1/2}]$$

It means that the velocity increases and decreases after the crest (see figure 18). The skin friction is extremal just before the crest, and there may be flow separation on the lee side. The behaviour is nearly the same than in the incompressible case but there is no influence of the bump before the beginning of it, it the incompressible case there was some small effect due to the Hilbert integral.

4.2.4 Bump on a flat plate in a Supercritical flow.

In the supercritical flow, the equation is the same for the edge velocity, but the story is completely different as $F > 1$. We observe a strong upstream influence on figure 19. The velocity decreases due to the bump, and the skin friction is negative upstream of the bump, the extremum is on the lee side, after the bump. There is a huge jump in $\tilde{\delta}_1$, a kind of hydraulic jump.

4.2.5 Wedge on a flat plate in a Supersonic flow.

As final example (fig 20), we present the results for the IBL on a flat plate with a wedge defined by $\bar{y}_w = \alpha(\bar{x} - 3.5)_+$; with α increasing by steps of 0.01 and $Re = 100000$. For enough large α we observe the "plateau" of pressure which is the signature of the self induced interaction and upstream influence. This increase of pressure before the wedge creates a region of reverse flow.

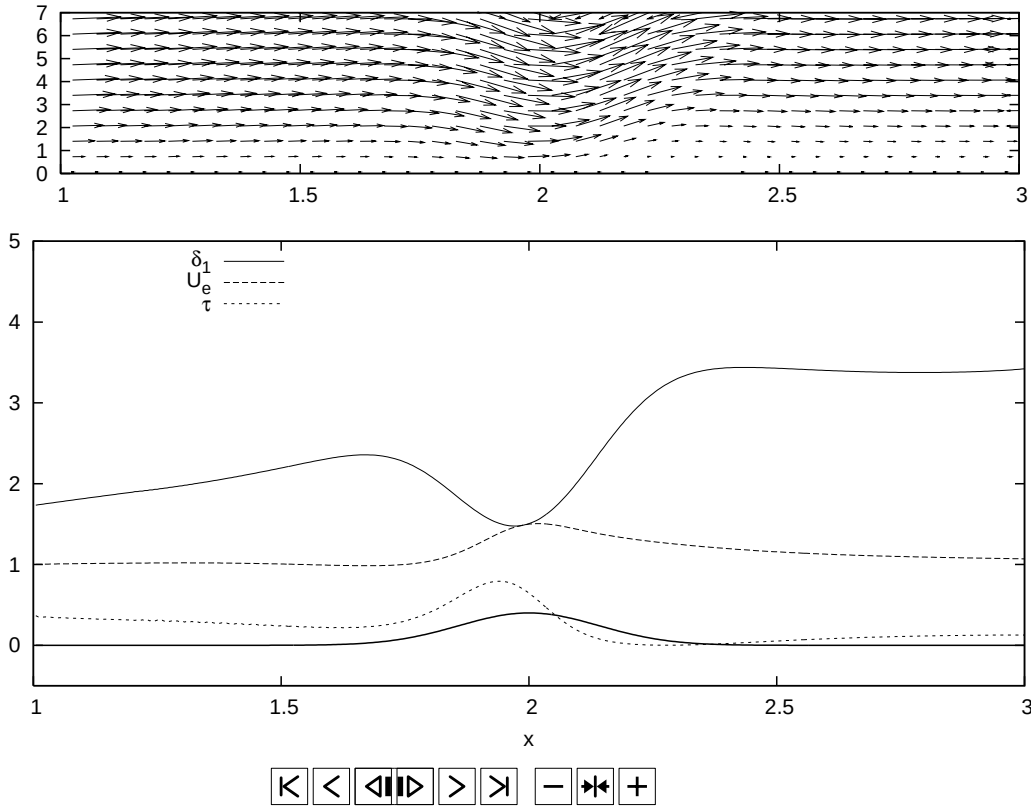

Figure 16: Incompressible flow [click to launch the movie, Adobe Reader required]. Top the velocity field $\tilde{u}, \tilde{v}$ (Prandtl transform), bottom the wall, here a bump, the displacement thickness $\tilde{\delta}_1$ (starting from Blasius value 1.7 in $\bar{x} = 1$), the skin friction (starting from Blasius value 0.3 in $\bar{x} = 1$) and the outer velocity starting from Ideal Fluid value 1 in $\bar{x} = 1$. A positive disturbance of the wall increases the velocity and decreases the displacement. Separation may occur after the bump, or before the tough.

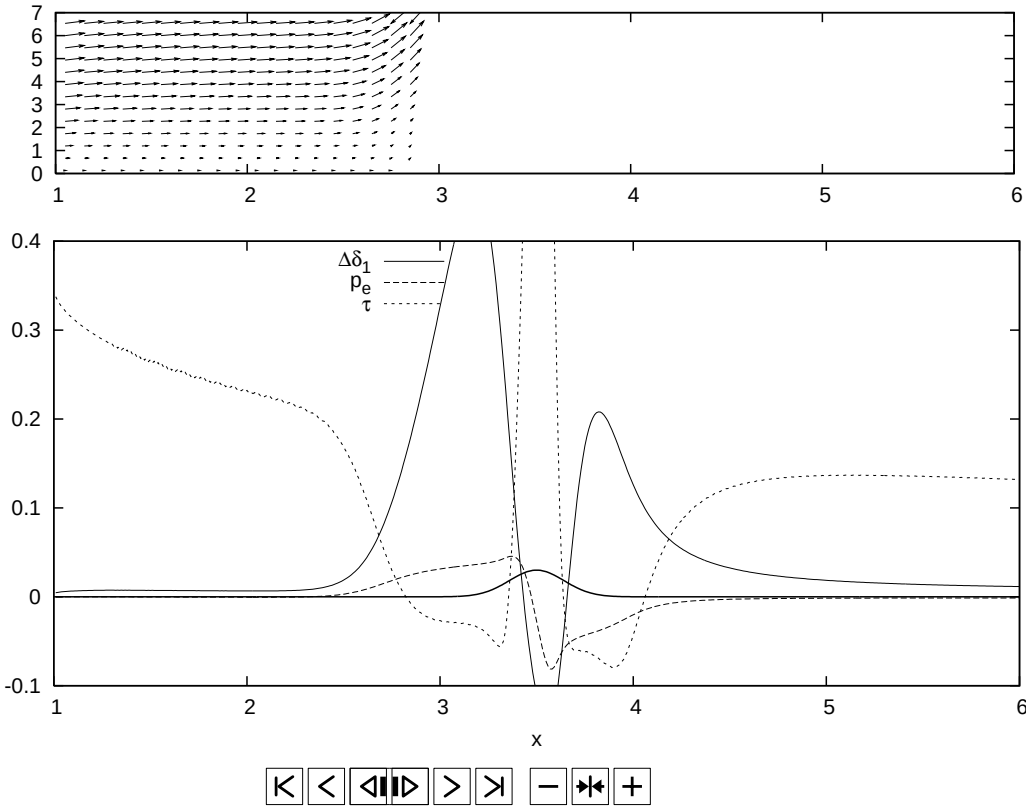

Figure 17: Supersonic flow on a flat plate with a bump [click to launch the movie, Adobe Reader required]. Top the velocity field $\tilde{u}, \tilde{v}$ (Prandtl transform), bottom the wall, here a bump, the perturbation of displacement thickness from Blasius $\Delta\tilde{\delta}_1$ (starting from 0 in $\bar{x} = 1$), the skin friction (starting from Blasius value 0.3 in $\bar{x} = 1$) and the outer pressure starting from Ideal Fluid value 0 in $\bar{x} = 1$. Note the pressure plateau associated to separation.

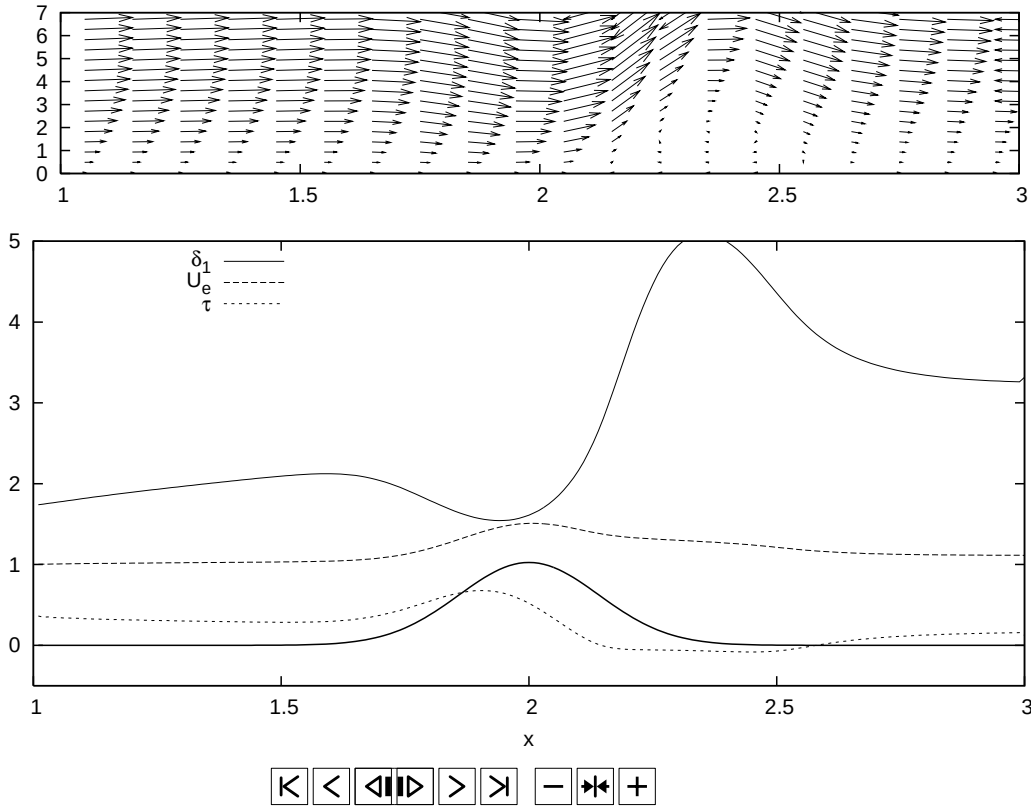

Figure 18: Subcritical flow on a flat plate[click to launch the movie, Adobe Reader required]. Top the velocity field $\tilde{u}, \tilde{v}$ (Prandtl transform), bottom the wall, here a bump, the displacement thickness $\tilde{\delta}_1$ (starting from Blasius value 1.7 in $\bar{x} = 1$), the skin friction (starting from Blasius value 0.3 in $\bar{x} = 1$) and the outer velocity starting from Ideal Fluid value 1 in $\bar{x} = 1$. A positive disturbance of the wall increases the velocity and decreases the displacement. Separation may occur after the bump.

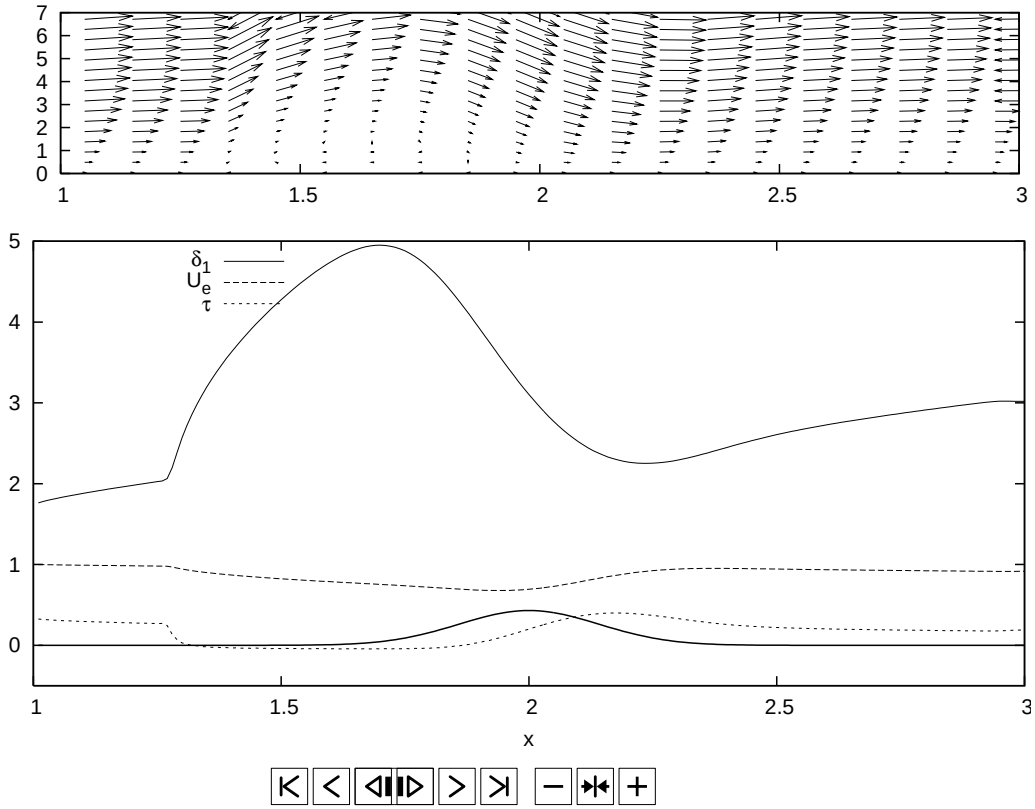

Figure 19: Supercritical flow on a flat plate [click to launch the movie, Adobe Reader required]. Top the velocity field $\tilde{u}, \tilde{v}$ (Prandtl transform), bottom the wall, here a bump, the displacement thickness $\tilde{\delta}_1$ (starting from Blasius value 1.7 in $\bar{x} = 1$), the skin friction (starting from Blasius value 0.3 in $\bar{x} = 1$) and the outer velocity starting from Ideal Fluid value 1 in $\bar{x} = 1$. A positive disturbance of the wall decreases the velocity and decreases the displacement. Separation may occur before the bump, note the long upstream influence.

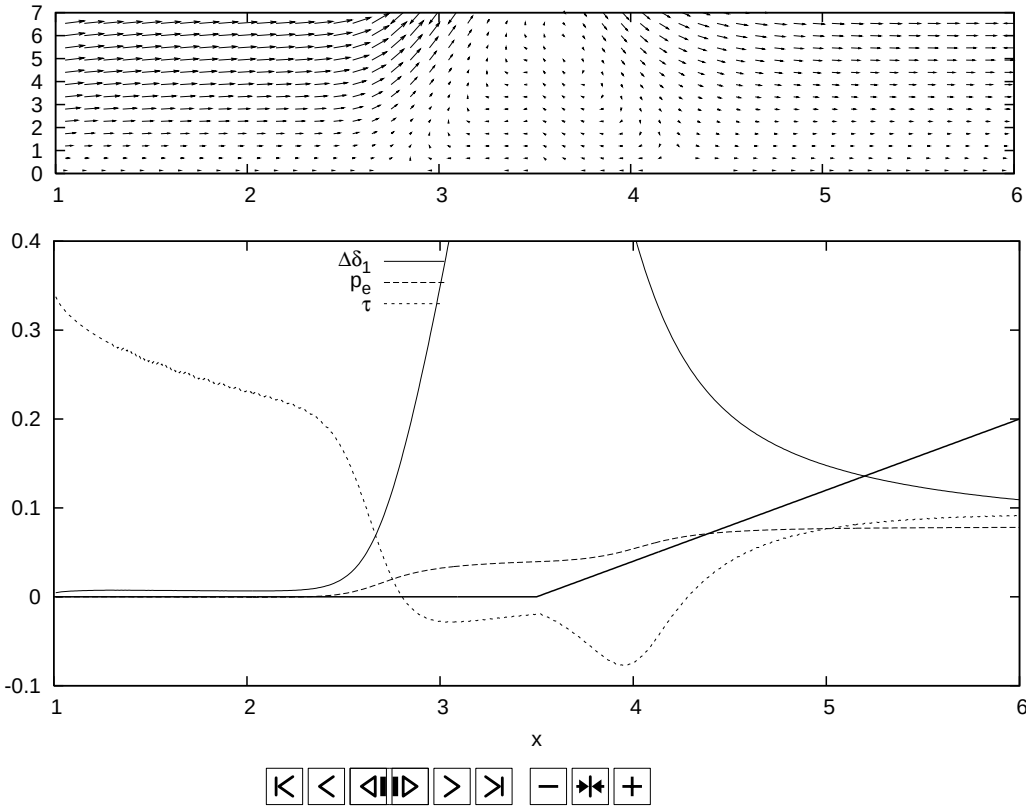

Figure 20: Supersonic flow on a flat plate with a wedge [click to launch the movie, Adobe Reader required]. Top the velocity field $\tilde{u}, \tilde{v}$ (Prandtl transform), bottom the wall, here a wedge in $\bar{x} = 3.5$, the perturbation of displacement thickness $\Delta\tilde{\delta}_1$ (starting from 0 in $\bar{x} = 1$), the skin friction (starting from Blasius value 0.3 in $\bar{x} = 1$) and the outer pressure starting from Ideal Fluid value 0 in $\bar{x} = 1$. Note the plateau pressure and the separation far upstream of the wedge.

4.2.6 Trailing edge

The trailing edge is such that at the position of it say $\bar{x}_{bdf}$, we have no more the no slip condition but the wake condition:

$$\bar{x} < \bar{x}_{bdf} : \quad \tilde{u}(\bar{x}, 0) = 0, \quad \bar{x} > \bar{x}_{bdf} : \quad \frac{\partial}{\partial \tilde{y}} \tilde{u}(\bar{x}, 0) = 0.$$

There is small upstream influence near the leading edge, in this region the velocity is increased to adjust to the new boundary condition.

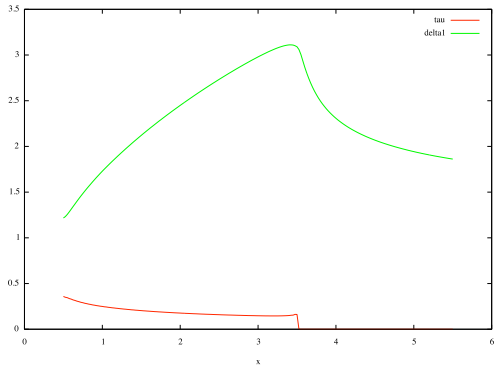

Figure 21: Example of trailing edge computation, $Re = 1.6\ 10^5$. The flat plate stops in $\bar{x} = 3.5$. The displacement thickness decreases in the wake, there is a singularity in the skin friction just before the trailing edge were the velocity adapts itself to the change on boundary condition.

4.3 An over simplified Model

4.3.1 von Kármán closure

The von Kármán equation contains interesting things, it reads for example:

$$\frac{d}{d\bar{x}}(\frac{\tilde{\delta}_1}{H}) + \frac{\tilde{\delta}_1}{\bar{u}_e}(1+\frac{2}{H})\frac{d\bar{u}_e}{d\bar{x}} = \frac{f_2 H}{\tilde{\delta}_1 \bar{u}_e},$$

with $\Lambda_1 = \tilde{\delta}_1^2 \partial \bar{u}_e/\partial \bar{x}$, we have

$$H = \left\{ \begin{array}{ll} 2.5905 e^{-0.37098\Lambda_1} & \text{if } \Lambda_1 < 0.6 \\ 2.074 & \text{if } \Lambda_1 > 0.6 \end{array} \right\}, \qquad f_2 = 1.05(-H^{-1} + 4H^{-2}).$$

Other closure exist.

4.3.2 Simple model

linearising in a crude simple way around the Blasius solution, so the gradient of velocity is small $\Lambda_1 << 1$ we develop the closure coefficients as $H = H_0 - Hp\Lambda_1 + ...$ and $f_2 = f_{20} + fp\Lambda_1 + ...$

with $\Lambda_1 = \tilde{\delta}_1^2 \partial \bar{u}_e/\partial \bar{x}$ and with $\bar{u}_e = 1 + \bar{u}$ and $\delta_1 = D(1-\tilde{A})\sqrt{\bar{x}}$ and $\bar{u}$ is the perturbation of the outer velocity and $-A$ is a perturbation of the displacement thickness.... so

$$\frac{HpD^2}{H_0^2}\frac{\partial^2}{\partial \bar{x}^2}\bar{u} + (1 + \frac{2}{H_0} - fpH_0 + Hpf_2 + \frac{3HpD^2}{2H_0^2})\frac{\partial}{\partial \bar{x}}\bar{u} + (\frac{1}{H_0} - \frac{f_2 H_0}{D})\bar{u} = \frac{1}{H_0}\frac{\partial}{\partial \bar{x}}\tilde{A} + (\frac{f_2 H_0}{D^2} + \frac{1}{H_0})\tilde{A}$$

the numerical values are $D = 1.7$, $H_0 = 2.5$, $Hp = .53$, $f_{20} = .25$ and $fp = 0.19$:

$$0.71\tilde{A} + .71\tilde{A}' = 0.35\bar{u} + 3.28\bar{u}' + 0.48\bar{u}''$$

this crude developement is such that, if now we introduce the ideal fluid relation between $\bar{u}$ and $-\tilde{A}$ we obtain or not upstream influence...

5 Conclusion

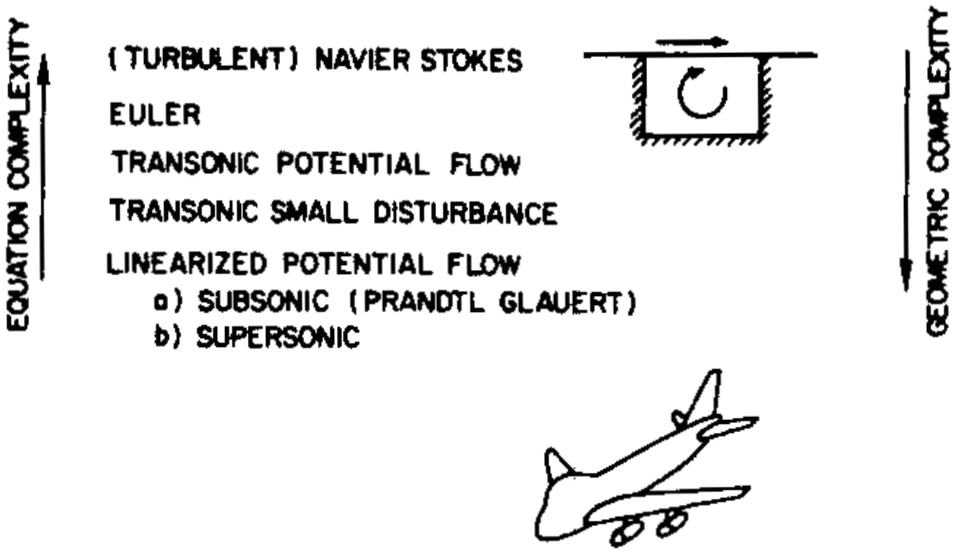

Figure 22: Complexity and models from Jameson [10]

So we now know that the boundary layer equations are more than useful. They can handle flow separation and compute reverse flow bubbles.

The methodology may be summarized in the figure 22 extracted from Jameson [10]. Even if this paper was written in 1983, it seems that most of the flying aircraft have been defined by Viscous Inviscid interactions. The Airbus A380 is one of the first aircraft designed with "full Navier Stokes" (in fact certainly crude RANS models). In the late 90', before the end of the century, a large effort has been done on Navier Stokes solvers. Lot of people are working on this equation. Tremendous progress have been done, and with Navier Stokes, the complexity of the geometry is a problem with lot of solutions. So Navier Stokes solvers are very promising, and give a lot of results.

To a certain extent, IBL-IVI methods are less versatile and require specific methods, they need a kind of "*savoir faire*" which as not been transmitted (Aftosmis et al. [1] point some difficulties of the IBL). For example Le Balleur has codes which may compute even large stall on wings, giving results very close to experiments. NS solver are not able to reproduce those results. Most of people who did all those IBL, IVI methods are now retired or nearly retired. A great part of IBL as been lost as people are focused now on Full Navier Stokes.

The review of Piomelli & Balaras [16], shows that up to now only very simple models are taken for boundary layer near the wall. They suggest a coupling of a LES Navier Stokes with a boundary layer code near the wall.

References

[1] Michael J. Aftosmis Marsha J. Berger, Juan J. Alonso, (2006) "Applications of a Cartesian Mesh Boundary-Layer Approach for Complex Configurations", 44th AIAA Aerospace Sciences Meeting, Reno NV, January 9-12, 2006 AIAA 2006-0652

[2] P. Bradshaw, T. Cebecci & J.H. Whitelaw (1981): "Engineering calculation methods for turbulent flow" Academic Press.

[3] D. Catherall and K.W. Mangler (1966) "The integration of the two-dimensional laminar boundary-layer equations past the point of vanishing skin friction. "J. Fluid Mech. 26 (1966) pp.163–182.

[4] Cebeci T. & Cousteix J. (1999): "Modeling and computation of boundary layer flows", Springer Verlag.

[5] Cousteix J., & Mauss J. (2006): "Analyse asymptotique et couche limite", Mathématiques et Applications, Vol. 56 2006, XII, 396 p.

[6] A. Dechaume, J. Cousteix, J. Mauss, An interactive boundary layer model compared to the triple deck theory, Eur. J. Mech. B Fluids 24 (4)(2005) 439 447

[7] Drela, M. and Giles, M. B. (1987). Viscous-inviscid analysis of transonic and low reynolds number flows. AIAA J., vol 25:1347–1355.

[8] R W Garvine (1968) " Upstream influence in Viscous Interaction Problems" Phys of Fluids V 11 N 7,pp 413 1423

[9] Kundu P.K. Cohen I.M. (2008) "Fluid Mechanics Fourth Edition", Academic Press.

[10] A. Jameson, The Evolution of Computational Methods in Aerodynamics. ASME J. Appl . Mech. 50 (1983) 1052-1070.

[11] Lees L. & Reeves B.L. "Supersonic Separated and reattaching Laminar Flows", AIAA Journal, Vol 2 11, 1964 pp 1907-1920.

[12] J.C. Le Balleur (1977), Couplage visqueux non-visqueux: Analyse du problème incluant décollements et ondes de choc. La Recherche Aérospatiale. no 6pp. 349-358.

[13] J.C. Le Balleur (1978), Couplage visqueux non-visqueux: Méthode numérique et applications aux écoulements bidimensionnels transsoniques et supersoniques. La recherche Aérospatiale. 1978-2, Eng Trans ESA TT-496 (1978), pp. 65–76.

[14] M. J. Lighthill (1953) "On Boundary Layers and Upstream Influence. II. Supersonic Flows without Separation" Proceedings of the Royal Society of London. Series A, Mathematical and Physical Sciences, Vol. 217, No. 1131 (May 21, 1953), pp. 478-507

[15] R. Lock and B. Williams. (1987) "Viscous-inviscid interactions in external aerody- namics. "Prog. Aerospace Science, 24:51–171, 1987.

[16] Piomelli U, Balaras E. (2002) "Wall-layer models for large-eddy simulations." Annual Rev. Fluid Mech. 34:349–74

[17] Reyhner, T.A. and & Flügge-Lotz, I., (1968). The interaction of a shock wave with a laminar boundary layer. Int. J. Non-linear Mech. 3, pp. 173–199.

[18] Stewartson K. (1964) "the Theory of Laminar Boundary Layers in Compressible Fluids", Oxford University Press, London (1964).

[19] Werle, M. J., ; Dwoyer, D. L., ; Hankey W. L., (1973) "Initial conditions for the hypersonic-shock/boundary-layer interaction problem." AIAA Journal 1973 0001-1452 vol.11 no.4 (525-530) doi: 10.2514/3.6780

[20] L.B. Wigton and M. Holt. (1981) "Viscous-inviscid interaction in transonic flow". AIAA-81- 1003, 1981.

The web page of this text is:
`http://www.lmm.jussieu.fr/~lagree/COURS/CISM/`

The last version of this file is on:
`http://www.lmm.jussieu.fr/~lagree/COURS/CISM/IVIIBL_CISM.pdf`